[논 문] 한국재료학회지
Korean Journal of Materials Research
Vol. 4, No. 3 (1994)

Bi-Sr-Ca-Cu-O계열 초전도체의 초구조

남궁 찬 · 이 상 윤*
육군제3사관학교 대학부 물리학과
*경북대학교 자연과학대학 물리학과

SUPERSTRUCTURES OF Bi-Sr-Ca-Cu-O SUPERCONDUCTORS

Chan Namgung and Sang Yun Lee*
Department of Physics, Korea Third Military Academy, Kyungpook, Youngchon, Kogyung, Changha, P.O. Box 135-9, Seoul, Korea, 771-849
**Department of Physics, Kyungpook National University, Taegu, Pook-gu, Sankyuk-dong, 1370, Korea, 702-701*

초 록 단일상(單一相)을 갖는 $Bi_2Sr_2CaCu_2O_{8+x}$(2212)의 x-ray 분말 pattern을 a=5.408, c=30.83A의 격자상수 및 역격자 벡터 $q^*=0.211b^*-c^*$을 갖는 pseudo-tetragonal subcell을 이용하여 모두 index 하였다. 임계온도 110K를 갖는 $Bi_2Sr_2Ca_2Cu_3O_{10+x}$상(相)은 incommensurate supercell에 속하는 매우 많은 x-ray분말선들을 가지고 있다. Indexing guide로 전자회절사진(electron diffraction photographs)을 이용 x-ray분말 pattern에 대한 지수결정방법을 얻었다.

$Bi_2Sr_2Ca_2Cu_3O_{10+x}$(2223)의 단위세포(unit cell)는 기하학적으로 격자상수 a=5.411, b=5.420, c=37.29(2) A을 갖는 orthorhombic subcell이다. Supercell반사 지수들은 subcell의 파 벡터 $\pm q^*=0.211b^*-0.78c^*$을 갖는 k, l 지수로부터 영향을 받은 것이다.

b방향으로의 incommensurate 성분 δ는 두 상(相)에 대해 다 같으나, 2212에서 2223 상(相)으로의 변환에 따라 c방향으로의 초격자성분(superlattic component)은 commensurate($\varepsilon=1$)로부터 incommensurate($\varepsilon=0.78$)로 변한다.

Abstract The x-ray powder pattern of single phase $Bi_2Sr_2CaCu_2O_{8+x}$ has been identified and fully indexed using a pseudotetragonal subcell with a=5.408, c=30.83 Å and an incommensurate supercell with reciprocal lattice vector, q*, given by $q^*=0.211b^*-c^*$. The x-ray powder pattern of the Pb-free 110K superconductor phase "$Bi_2Sr_2Ca_2Cu_3O_{10+x}$" has many lines which belong to an incommensurate supercell. Using electron diffraction photographs as a indexing guide, an indexing scheme for the powder pattern has been obtained. The unit cell has a geometrically orthorhombic subcell a=5.411, b=5.420, c=37.29(2) Å. Supercell reflections have indices that are derived from the subcell k, l indices by addition of $\pm q^*$, where $\pm q^*=0.211b^*-0.78c^*$.

The incommensurate component in the b direction, δ, is the same for both phases but on going from 2212 to 2223 phase, the superlattic component in the c direction changes from commensurate($\varepsilon=1$) to incommensurate($\varepsilon=0.78$).

1. Introdution

The Bi-Sr-Ca-Cu-O system contains a number of superconducting phases in a homologous series $Bi_2Sr_2Ca_{n-1}Cu_nO_{2n+4+x}$ with n=1, 2 and 3. These phases $Bi_2Sr_2CuO_{6+x}$, $T_c\sim20$ K [1], $Bi_2Sr_2CaCu_2O_{8+x}$, $T_c\sim80$K [2,3], and $Bi_2Sr_2Ca_2Cu_3O_{10+x}$, $T_c\sim110$K [4,5] referred to as 2201, 2212 and 2223 phases respectively, are closely related to each other. The structures of the ideal members of the homologous series are based on alternating Bi_2O_2 and Sr-CuO_2-SrO layers. Figure 1 illustrates the ideal unit cells of $Bi_2Sr_2Ca_{n-1}Cu_nO_{2n+4+x}$, with n=1, 2, and 3. Various structural studies on these

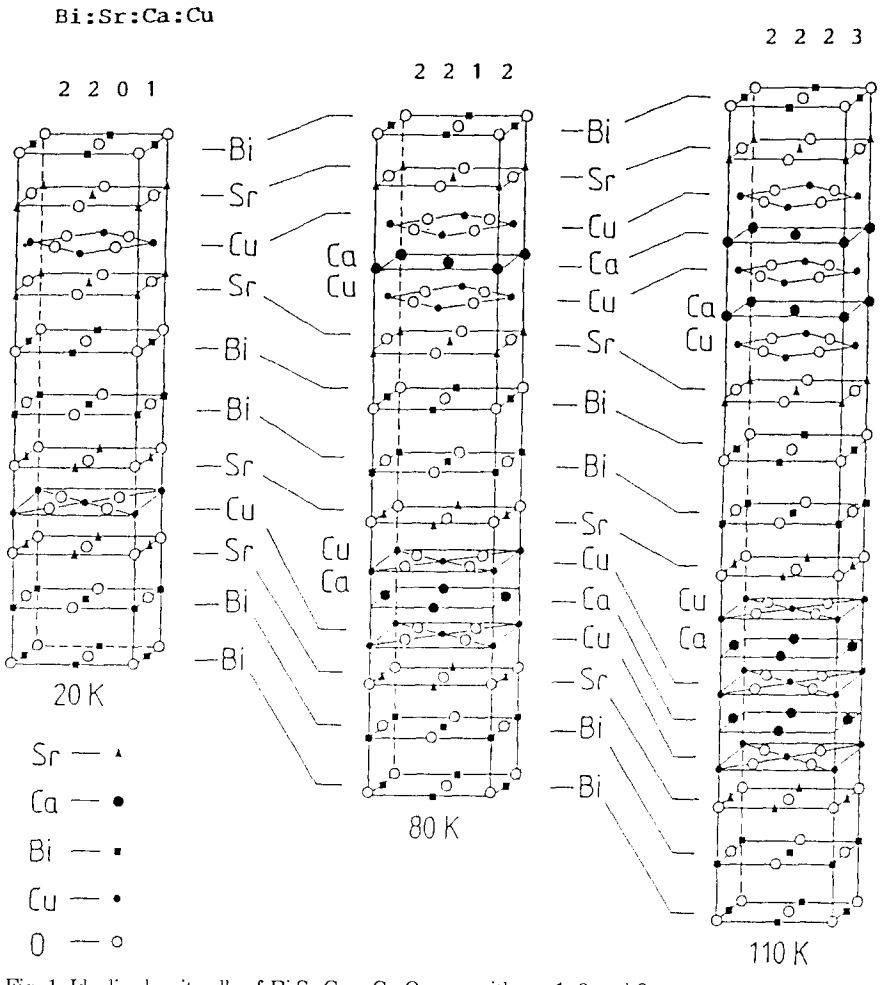

Fig. 1. Idealized unit cells of $Bi_2Sr_2Ca_{n-1}Cu_nO_{2n+4-x}$ with n=1, 2 and 3.

phases have been reported, as follows ;

(1) $Bi_2Sr_2CaCu_2O_{8+x}$: this phase has been investigated by powder x-ray diffraction[2,6,7], single-crystal x-ray diffraction[2,3], electron diffraction[2,3,8~11], high resolution electron microscopic imaging [2,12~19] and powder neutron diffraction[20].

The average structure has an orthorhombic unit cell with dimensions of a~5.4 Å, b~5.4 Å and c~30.8 Å. Electron diffraction studies of this phase reveal a long period superstructure in the b direction which appears to be incommensurate[2,3,8~11]. A more extensive examination of the reciprocal lattice[8] showed that the superstructure is not only incommensurate in b but also has an additional, commensurate component in c[8] and that the superlattice wave vector, q*, was given by q*= (0, 1/4.7, 1). Various structural origins of the superstructure of 2212 phase has been proposed, but it is far from clear which model is correct. These are :

(a) Ordering of Bi depleted zones[20] ; a superstructure model involving ordering of Bi depleted and Bi enriched zones was proposed by Matsui et al. They suggest that there is either a periodic replacement of Bi by Sr and/or Ca atoms accompanied by lattice distortions, or that only distortions of the Bi site occurs without atom replacement.

(b) Additional oxygen in the BiO planes[21] ; it has been suggested that the origins of the superstructure are displacement of Bi cations associated with a small number of additional

oxygen atoms in the BiO layers.

(c) Rotational distortions of the (BiO_6) octahedra[8] ; it was suggested by Chen et al that the superlattice is due to some kind of rotational distortions of the Bi-O octahedra with respect to the a axis. The presence of the c component in the superlattice wave vector requires that the $Bi-O_6$ octahedra above and below the Ca layer tilt in opposite directions. This could be related to the unusual bismuth coordination. Although the oxygen atoms around this site form a slightly distorted octahedron, the lone pair of electrons on the bismuth ions (Bi^{3+}) generally give rise to much less symmetric environments. It is also possible that distortions that lower the site symmetry could lead to buckling of the BiO layers to form a superstructure associated with periodic displacements[22].

(d) Layer misfit structure composed of 19 Cu pairs commensurate with 20 Bi pairs[10] and a sinusoidal displacement of Bi, Sr in b, c directions and of Cu in the c direction only[19].

(e) Sunshine et al suggest that the superlattice could be due to the presence of and ordering of Sr or Bi in the Ca site with oxygen incorporation to complete its coordination sphere. There is a clear indication from structural refinements that additional electron density is present on the Ca site and possibly at the vacant oxygen sites in that layer[23].

(f) Hu et al[24] suggest that of the several types of superstructure models, only the model with additional oxygen in the BiO planes was found to fit all the structural data. Therefore, they proposed a model that consists of a periodic addition of one in ten oxygen atoms in the BiO planes giving a formula of $Bi_2Sr_2CaCu_2O_{8.2}$ and a displacement of the surrounding atoms.

Powder x-ray diffraction data have been reported for $Bi_2Sr_2CaCu_2O_{8+x}$, indexed on an orthorhombic cell, $a=5.410\pm0.003$, $b=5.439\pm0.005$, $c=30.78\pm0.03$ Å[2]. This indexing scheme did not involve use of the supercell along b, which was given as 27.2 Å, 5 times the subcell repeat. In the powder x-ray patterns reported by several authors[2,25] for this compound, several rather strong peaks have been left unindexed. Since a polycrystalline sample is unusually identified by the powder x-ray diffraction method, it is very important to check if those extra peaks are due to the satellite reflections or due to an impurity phase.

(2) $Bi_2Sr_2Ca_2Cu_3O_{10+x}$; electron diffraction and high resolution electron microscopy have been used to study the modulated structure of the 110K superconducting phase[15,17]. Structural determination indicates that the crystal is incommensurate in at least one direction and that the average structure has a pseudo tetragonal unit cell with cell dimensions $a=5.41$ Å and $c=36.38$ Å. The structural modulation is mainly caused by the displacements of Bi atoms in the BiO planes as described above for the origins of superstructure in the 2212 phase.

X-ray powder data for single phase 2223, without Pb doping, have not been reported previously. Tallon et al[26] reported the effects of Pb-substitution for Bi in the homologous superconducting series for nearly single phase n=3, in which the x-ray powder diffraction pattern was indexed using a pseudo tetragonal unit cell with $a=5.410$ and $c=37.124$ Å. The following two points are important issues ; whether the crystal structure of the Pb-substituted sample is the same as that of the Pb-free one, and where the Pb atoms are located in the crystal structure. Hiroshi et al[27] observed the Pb atoms using high resolution transmission electron microscopy (HRTEM) in which Pb atoms were located in the Bi-O layers with an atomic ratio of Pb to Bi of 0.1 but the modulated structure along the b axis was the same as in the case of a Pb-free sample. This results indicates that the crystal structure of the Pb-doped sample appears to be the same as that of Pb free sample. Recently, a calculated powder pattern was generated based on the analogous structure of

the T1-2223 phase and lattice parameters given by Zandbergen et al[29]. Powder x-ray diffraction data have been reported for the Pb doped 2223 phase, $Bi_{1.9}Pb_{0.35}Sr_2Ca_2Cu_3O_{10+x}$, indexed on a pseudo-tetragonal cell with $a=5.410$Å and $c=37.124$Å by Tallon et al[26]; however, there are no good reported experimental data for 2223 phase. One objective in this work has been to prepare such data and index them. Like the 2212 phase, materials with $n=3$ exhibit a $5.4*5.4$Å subcell in the basal plane with the same 19/4 incommensurate superlattice in the b* direction[30,31]. The incommensurate $\sim 1/5b^*$ component probably has similiar origins to those suggested in the 2212 phase.

In this work, x-ray powder diffraction studies of single phase 2212 samples and samples of composition 2224 containing predominatly the 2223 phase are presented.

Ⅱ. Calculation of subcell and supercell d-spacings

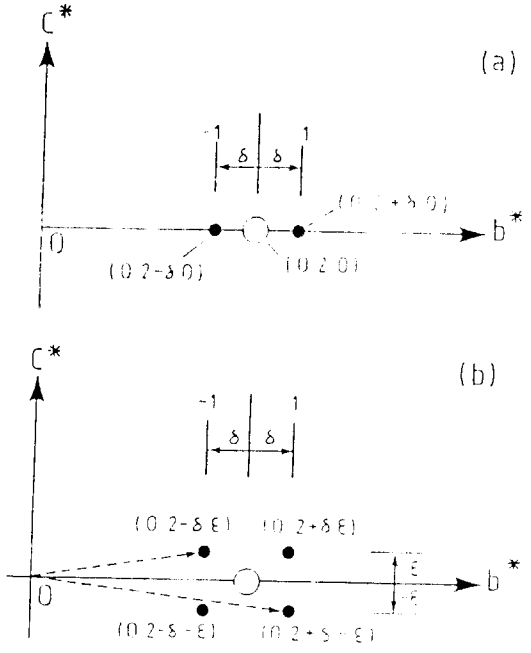

Fig. 2. Schematic diagrams of satellite reflections on the (0, k, 1) reciprocal plane. Open circles indicate the reflections from subcell, while solid circles locate the incommensurate superlattice reflections.

Figure 2 shows schematic of satellite reflections in the (0 k 1) reciprocal lattice plane. Open circles indicate the reflections from the subcell, while solid circles locate the superlattice reflections. Satellite spots appear on either side of the supercell positions in the reciprocal lattice.

Subcell and supercell d-spacings are calculated using the following equations.

For subcell :

$$1/(d_{sub})^2 = h^2/a^2 + k^2/b^2 + l^2/c^2$$

For supercell :

$$1/(d_{sup})^2 = h^2/a^2 + (k-\delta)^2/b^2 + (l-\varepsilon)^2/c^2$$

$$1/(d'_{sup})^2 = h^2/a^2 + (k+\delta)^2/b^2 + (l+\varepsilon)^2/c^2$$

Where the superlattice has vector $q^* = \delta b^* + \varepsilon c^*$, $0<\delta<1$. For each subcell d spacing, the two supercell d spacings corresponding to $\pm q^*$, are given as d^- and d^+. Procedures used for indexing supercell reflections are given in the results section.

Ⅲ. Experiments

(1) Sample preparations

$Bi_2Sr_2CaCu_2O_{8+x}$ (2212 phase) ; samples with starting composition $Bi_2Sr_2CaCu_2O_{8+x}$ were prepared by solid state synthesis. The starting materials were Bi_2O_3, $SrCO_3$, $CaCO_3$ and CuO. Prior to weighing, the CuO was dried at 700℃ and the other reagents were dried at ~500℃ for more than 4 hours. Stoichiometric quantities totalling ~5g were weighed, mixed, dried and reacted in gold foil crucibles at 700 ~800℃ for 24~48 hours. They were then removed from the furnace, reground to obtain a homogeneous mixture, made into pellets to increase reaction rate and refired at 880℃ for 48~72 hours. After reaction at 880℃ for 18 ~72 hours the pellets were removed, crushed, repelleted and fired at 880℃ for a further 72 hours in air. These long heating times were required to ensure complete elimination of the 2201 phase, $Bi_2(SrCa)_2CuO_{6+x}$.

$Bi_2Sr_2Ca_2Cu_3O_{10+x}$; Samples of nominal compositions, $Bi_2Sr_2Ca_2Cu_3O_x$ (2223 phase) and

$BiSrCaCu_2O_x$(1112 phase), were prepared by solid state synthesis from mixtures of Bi_2O_3, $SrCO_3$, $CaCo_3$ and CuO. The mixtures were heated at 850℃ for 24 hours followed by further grinding and pelleting. Next, they were sintered in air in the temperature range 870~900℃ for 7 to 30 days.

(2) X-ray powder diffraction study

Phase identification of the samples and accurate d-spacing measurements were carried out by x-ray powder diffraction using a Phillips Hagg Guinier model XDC-700 powder camera, $Cu_{K\alpha 1}$, radiation. The procedure for indexing powder patterns and determination of unit cell dimensions was carried out using a least square programme, POWCAL, LSQC and DSPC in Aberdeen University of U.K.

Ⅳ. Incommensurate structure and x-ray powder diffraction data for $Bi_2Sr_2CaCu_2O_{8+x}$

It was found that the x-ray powder pattern of the 2212 phase always contained lines that could not be indexed on the orthorhombic subcell. These extra lines that could not be indexed on the orthorhombic subcell. These extra lines are shown arrowed in figure 3. They were attributed to the supercell and, with the aid of electron diffraction photographs as an indexing guide, the complete pattern could be indexed accordingly.

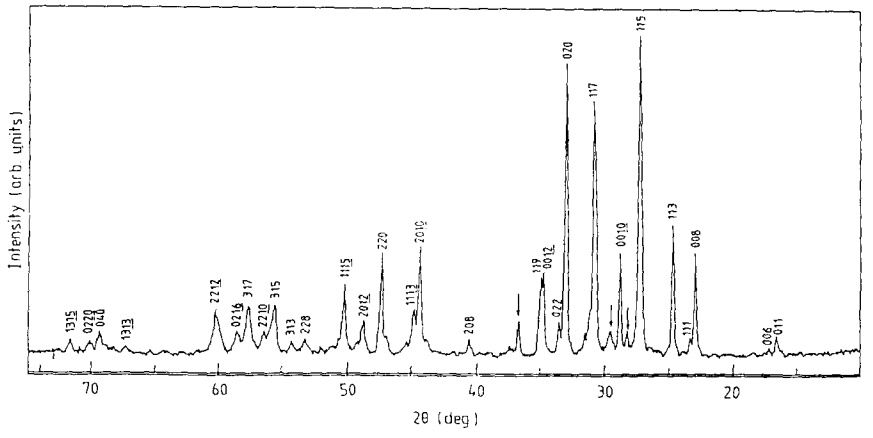

Fig. 3. Powder x-ray diffraction pattern of $Bi_2Sr_2CaCu_2O_{8+x}$, showing the presence of extra lines (arrowed) that can not be indexed using the orthorhombic subcell.

Electron diffraction photographs of the a*b* plane of the reciprocal lattice, figure 4, showed the incommensurate supercell parallel to b*, similar to that reported by othres[2,3,6,8~10]. Starting with the 020 reflection, which is one of the strongest low angle lines in the x-ray powder pattern, the nearest satellite spots in the electron diffraction pattern were, initially, assigned the indices (0 $2\pm\delta$ 0). Their seperations from the subcell 020 refleection were measured and was estimated as 0.21. The positions of the two corresponding lines in the powder x-ray diffraction pattern were then calculated to be 2.44 Å ($2\theta=36.8°$) and 3.02 Å (29.6°) and coincided approximately with two of the unindexed lines arrowed in figure 3.

(i) In order to make a more accurate determination of δ and confirm the indexing of these two powder lines, their positions were measured accurately and the reverse calculation made, to give δ for each.

$$1/(d^-_{sup})^2=h^2/a^2+(k-\delta)^2/b^2+(1-\varepsilon)^2/c^2 \quad (1)$$

$$1/(d^+_{sup})^2=h^2/a^2+(k+\delta)^2/b^2+(1+\varepsilon)^2/c^2 \quad (2)$$

The calculation was carried out using equation (1) and (2).

For $\delta=0.25(\varepsilon=0)$

$$1/(d^-_{sup})^2=(0)^2/(5.41)^2+(2-0.25)^2/(5.41)^2+(0)^2/(30.82)^2$$

$$d^-_{sup}=3.091\text{A}$$

$$1/(d^{-}_{sup})^2 = (0)^2/(5.41)^2 + (2+0.25)^2/(5.41)^2 + (0)^2/(30.82)^2$$

$$d^{+}_{sup} = 2.404\,A$$

Table 1. Supercell d spacings (A) about (0 2+δ 0) and (0 2−δ 0) for each given δ value

k	· δ	d_{sup}(Å)	d^{+}_{sup}(Å)
4	0.25	3.0914	2.4044
5	0.20	3.0055	2.4590
6	0.167	2.9509	2.4969

(ii) The calculated supercell d spacings (table 1) were plotted against the given δ values (0.25, 0.20, 0.167) (figure 5).

(iii) The apparent δ values from figure 5 for the two 020 satellite lines are significantly different and indicate that the indexing scheme cannot be correct.

Since the δ value obtained by electron diffraction was measured from photographs of the a*b* plane, it was next considered possible that the superstructure had a component in the c̲ direction, which would not have been evident from the a*b* projection. The two satellites were then assigned indices (0 2 ± ∓ 1), in accord also with electron diffraction

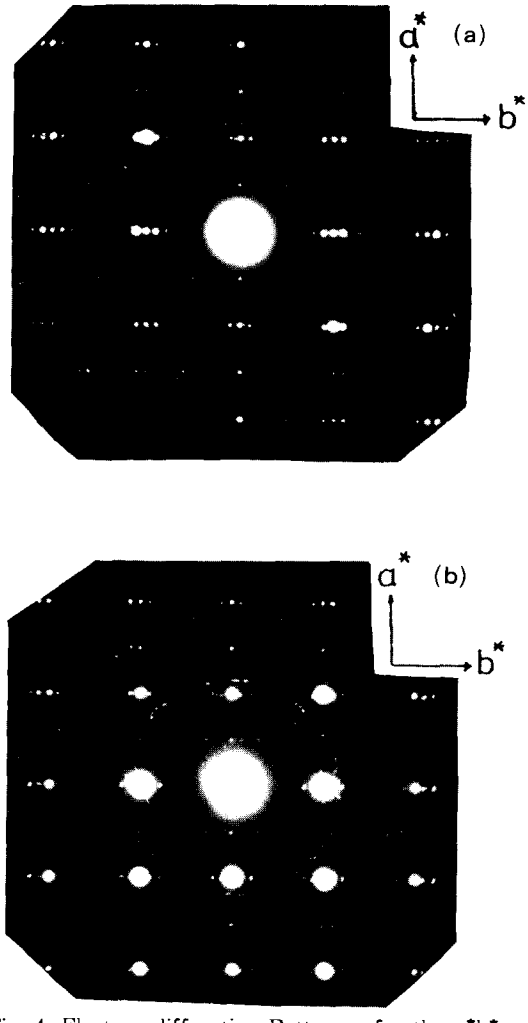

Fig. 4. Electron diffraction Patterens for the a*b* plane for (a) sample annealed at 400℃ and (b) sample annealed at 830℃ in air.

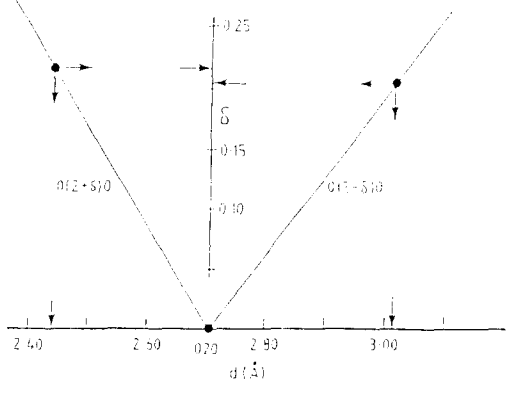

Fig. 5. Unsuccessful attempt at indexing supercell lines by taking account of incommensurate superstructure in b.

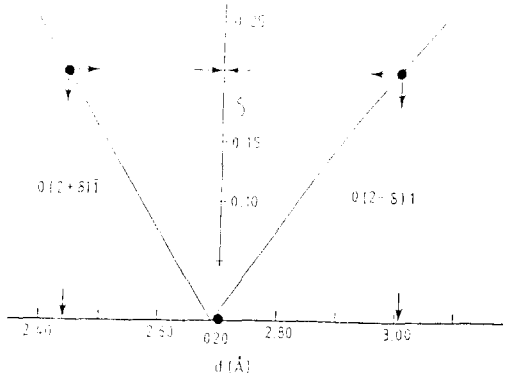

Fig. 6. Successful attempt at indexing supercell lines by taking account of incommensurate supercell in b̲ and commensurate supercell in c̲.

results that showed the superstructure to have a commensurate component in c as well as the incommensurate component in b[8].

The procedure for obtaining a more accurate δ value using this scheme was carried out as described below :

(i) The d spacings (Å) for the supercell lines were calculated using equation (1) and (2) in order to plot against δ values, 0.25, 0.20 and 0.167. The results are listed in Table 2.

Table 2. Supercell d spacings (Å) about (0 2±δ ∓1) for a given δ value.

k	δ	d^-_{sup}(Å)	d^+_{sup}(Å)
4	0.25	3.0760	2.3970
5	0.20	2.9913	2.4513
6	0.167	2.9380	2.4884

(ii) The calculated supercell d spacings (table 2) were plotted against (figure 6).

(iii) The δ values for the two 020 stellites were found to be in excellent agreement as shown in figure 6, with a value δ=0.211.

Since two of the unidexed lines in figure 3 could be indexed satisfactorily on the supercell, it is highly likely that other powder lines will also appear that depend on the supercell. Two possible situations were considered for their indexing. One in which the supercell lines have indices (h, k+δ, l+1), (h, k−δ, l−1) and the other with indices (h, k+δ, l−1), (h, k−δ, l+1). These two possibilities are indistinguishable for the 020 reflection but for reflections with non-zero l values, the two possibilities give rise to two different sets of d spacings. Comparison of calculated d spacing for the supercell reflections associated with the three strongest subcell reflections 020, 115 and 117, table 3, with the observed powder pattern indicates the latter scheme to be correct.

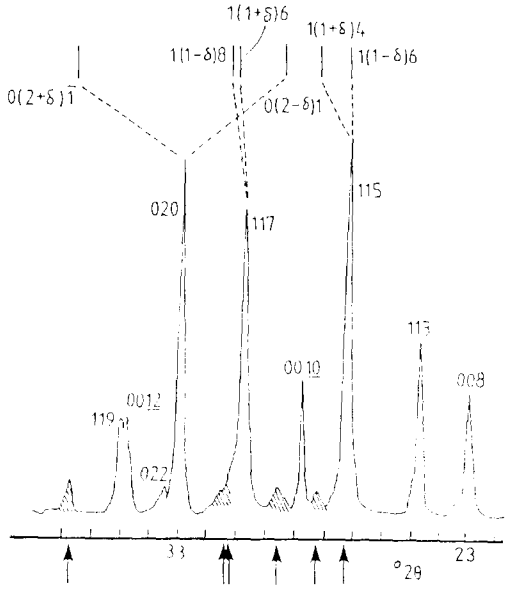

Fig. 7. Part of fully indexed powder pattern showing subcell and supercell reflections.

The positions of the most prominent superlattice lines are indicated in figure 7. All of the extra lines and shoulder peaks can be indexed by considering the satellites about the three strongest lines, 020, 115, and 117. It is likely that many other powder lines are present that were too weak to be observed by our techniques but which would be detected using high intensity x-ray (or neutron)

Table 3. Calculated subcell and possible supercell d spacings (Å), for the three strongest x-ray powder diffraction reflections. Equations 1 and 2 are used for calculating d^+_{sup} and d^-_{sup}, the pair of supercell reflections corresponding to $\pm q^*_2$.

		$q^*_1 = b^* + c^*$		$q^*_2 = b^* - c^*$	
h k l	d_{sub}	d^+_{sup}	d^-_{sup}	d^+_{sup}	d^-_{sup}
0 2 0	2.7052	2.4392	3.0096	2.4392	3.0096
1 1 7	2.8886	2.5686	3.2741	2.8615	2.8545
1 1 5	3.3511	2.8615	3.7201 +	3.1451	3.2741

+ has no counterpart in the observed powder pattern.

Table 4. Powder diffraction pattern for the $Bi_2Sr_2CaCu_2O_{8+\delta}$ (2212) superconductor, based on a subcell $5.410 \times 5.410 \times 30.84$ Å.

h	k	l	d(obs)	d(cal)	I/I(obs)	I/I(cal)
0	0	2	15.5	15.4	14	19
0	1	1	5.34	5.33	3	2
0	0	6	5.16	5.14	1	0
0	0	8	3.861	3.855	26	22
1	1	1	3.801	3.797	3	4
1	1	3	3.591	3.586	35	24
1	(1−δ)	6		3.2741		
1	1	5	3.2530	3.2511	100	100
1	(1+δ)	4	3.1471	3.1451	5	
0	0	10	3.0854	3.0837	25	11
0	(2−δ)	1	3.0116	3.0096	6	
1	1	7	2.8913	2.8886	77	53
1	(1+δ)	6	+	2.8615		
1	(1−δ)	8	+	2.8545		
0	2	0	2.7064	2.7052	74	48
2	0	0				
0	2	2	2.6658	2.6645	8	5
2	0	2				
0	0	12	2.5709	2.5698	25	8
1	1	9	2.5545	2.5524	20	15
0	(2+δ)	1	2.4397	2.4392	6	
2	0	8	2.2166	2.2143	2	5
0	2	8				
2	0	10	2.0326	2.0336	28	16
0	2	10				
1	1	13	2.0123	2.0160	9	5
2	2	0	1.9118	1.9129	26	16
2	0	12	1.8625	1.8632	7	5
0	2	12				
1	1	15	1.8115	1.8109	20	9
2	2	8	1.7136	1.7135	3	3
3	1	3	1.6877	1.6877	1	2
1	3	3				
3	1	5	1.6491	1.6487	15	11
1	3	5				
2	2	10	1.6254	1.6255	5	3
3	1	7	1.5946	1.5949	17	8
1	3	7				
0	2	16	1.5735	1.5697	6	2
2	0	16				
2	2	12		1.5344		3
1	3	9	1.5323	1.5305	15	5
3	1	9				
1	3	13	1.3874	1.3877	2	1
3	1	13				
0	4	0	1.3530	1.3526	4	3
4	0	0				
0	2	20	1.3397	1.3396	1	2
2	0	20				
1	3	15	1.3150	1.3151	1	3
3	1	15				

+Shoulder peaks were observed beside the 117 line at 2.8913 Å but their d spacings and intensities could not be accurately measured.

sources. Electron diffraction photographs show the presence of superlattice reflections about every subcell reflection and in some cases, higher order supercell reflections have significant intensity and might be expected to appear in the x-ray powder pattern.

The relative positions of the superlattice lines depend very much on the h k l values of the parent, subcell lines. Thus, for the 020 line the supercell lines appear on either side of the subcell line in the powder pattern ; for the 115 lines, one satellite line coincides with the subcell line and one occur at lower d spacings whereas for the 117 lines, both satellites occur to the same side of the subcell line.

An indexing scheme for the complete, observed powder pattern is given in table 4. Although the symmetry of both subcell and supercell is orthorhombic, the a and b parameters of the subcell are so similiar that the subcell has been treated as geometrically tetragonal. Many x-ray powder lines, which should appear as closely spaced doublets, e.g. 020 and 200, appear as singlets. The only subcell line in table 4 which belongs uniquely to the orthorhombic cell is 011 since 101 is systematically absent. The calculated intensities given in table 4 were based on a crystal structure determination of the subcell[3]. There is satisfactory agreement between observed and calculated intensities for the subcell lines.

Figure 4 shows the electron diffraction patterns for samples of $Bi_2Sr_2CaCu_2O_{8+x}$ annealed at 400 and 830℃ in air to give excess oxygen contents, x, determined by titrimetry as 0.190 and 0.178, repectively and with superconducting transition temperatures of 73 and 87K. Spot sizes are different due to diffrent crystal thickness ; however, no significant differences in the electron diffraction patterns were seen, figure 4, nor any detectable shifts in the value of δ determined from the x-ray powder pattern. It is unusual that so many satellite reflections are observed in a powder pattern and that one of them $(1, 1-\delta, 6)$ is quite strong.

In summary, the x-ray powder diffraction pattern of single phase $Bi_2Sr_2CaCu_2O_{8+x}$ has been identified and fully indexed using a pseudo-tetragonal subcell with $\underline{a}=5.408$, $c=30.83$ Å and an incommensurate supercell with reciprocal lattice vector, q* given by $q^*=0.211b^*-c^*$. For samples with different oxygen stoichiometry x, q* is essentially constant ; therefore the incommensurability appears not to be connected directly with oxygen content.

V. Superstructure and x-ray powder diffraction data for the 110K phase.

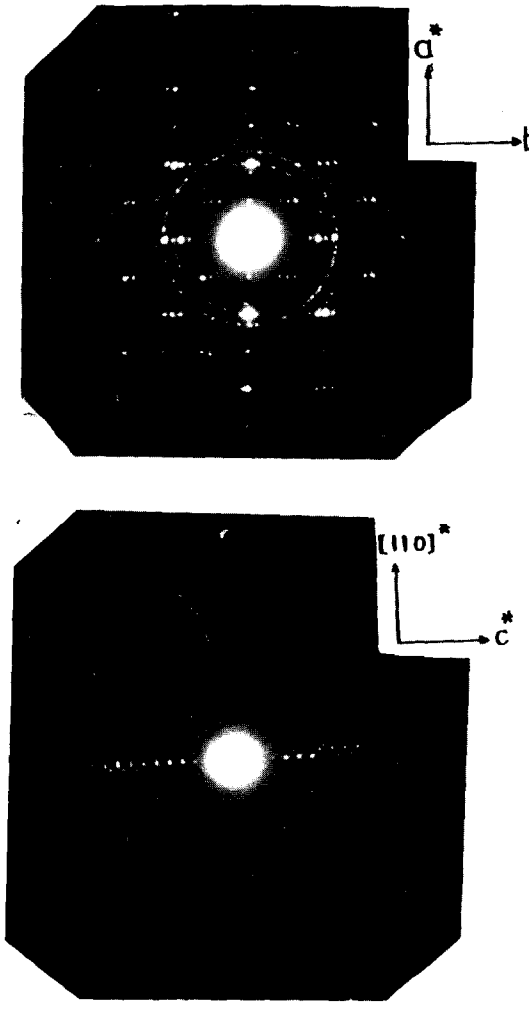

Fig. 8. Electron diffracion Patterns for the (hk0) and (hh1) reciprocal lattice planes for samples annealed jat 880℃ in air for 30 days.

Table 5. Powder diffraction pattern for the Bi-Sr-Ca-Cu-O (2223) superconductor, based on a subcell 5.410×5.420×37.29 Å

					Diffractometer		
h	k	l	q	d(Hägg)	d(cal)	I	d(cal)
0	0	2		18.8128			18.6430
0	1	1		5.3811	5.3545	4.7	5.3640
1	1	1		3.8032	3.7976	4.0	3.8094
0	1	7					3.7991
1	1	3		3.6641	3.6670	5.2	3.6596
0	1	7	+1	3.5945	3.5882	4.7	3.5884
1	1	1	+1	3.4556	3.4507	18.8	3.4494
1	1	5		3.4110	3.4124	13.4	3.4065
1	1	3	+1		3.3754	4.8	3.3796
0	2	2	−2	3.2536	3.2527	7.7	3.2538
1	1	5	+1	3.2173	3.2135	6.3	3.2139
1	1	7		3.1117	3.1075	9.7	3.1093
0	0	12					3.1072
0	2	0	−1	3.0024	3.0099	17.4	3.0218
1	1	5	+2				2.9972
1	1	7	+1		2.9843	7.8	2.9903
1	1	9	−1		2.8294	6.6	2.8375
1	1	9		2.7991	2.8003	40.5	2.8121
0	0	14	+1				2.8040
0	2	0		2.7039	2.7125	100	2.7101
0	2	2			2.6879	27.4	2.6819
0	0	14		2.6625	2.6624	23.6	2.6633
2	0	4	+1	2.6267	2.6233	3.3	2.6204
2	0	4		2.5993			2.5982
2	0	4	−1		2.5573	5.3	2.5432
0	1	13		2.5368	2.5389	11.1	2.5351
2	0	6		2.4803			2.4806
0	2	0	+1	2.4444	2.4455	8.1	2.4492
0	2	10		2.1975	2.1947	5.3	2.1922
2	0	12	+2	2.1284	2.1275	3.8	2.1269
0	2	10	+1	2.1056	2.1115	5.1	2.0970
2	0	12		2.0376	2.0380	12.4	2.0404
2	2	4	−2		2.0285	5.0	2.0249
2	2	0	−1		2.0181	6.0	2.0154
2	0	12	−1	1.9769			1.9778
2	2	4	−1	1.9552	1.9542	10	1.9530
2	2	0		1.9168	1.9164	36.5	1.9147
1	1	17			1.9045	7.3	1.9032
2	0	14		1.8927	1.8949	7.2	1.8980
2	2	4		1.8698			1.8755
2	2	0	+1		1.8152	10.5	1.8156
0	3	3		1.7844	1.7832	3.5	1.7879
2	0	14	−2	1.7771			1.7767
2	1	15		1.7354			1.7342
3	1	5		1.6679			1.6680
3	1	7		1.6308	1.6292	3.8	1.6293
1	1	21			1.6100	3.8	1.6293
3	0	12	+2	1.6033	1.6012	7.7	1.5974
1	3	11			1.5302	5.8	1.5294
0	3	13		1.5285	1.5254	4.7	1.5287
0	4	0		1.3544			1.3551
0	0	28		1.3304			1.3316
2	3	13					1.3309

*Supercell vector $\mathbf{g}^*$ is given by $q^* = 0.21b^* - 0.78c^*$.

The electron diffraction patterns of the (hkO) and (hh1) planes of the reciprocal lattice (figure 8) show an incommensurate supercell in the b and c directions, similiar to that of the 2212 phase ($Bi_2Sr_2CaCu_2O_{8+x}$) and reported by others[26]. The distance, δ, from the main subcell 020 reflection to the first order satellite reflection was measured and δ was found approximately to be 0.208. The incommensurate component along c could be seen from the electron diffraction photographs (figure 8). The superlattice periodicity along the c axis, ε, was measured from the (hh1) plane as approximately 0.75 showing the supercell to be incommensurate along c.

Indexed powder x-ray diffraction data are given in table 5. The x-ray powder diffraction pattern could be indexed using an orthorhombic subcell, $a=5.410(9)\pm0.002$, $b=5.420(2)\pm0.002$ and $c=37.29\pm0.02$ Å, with a supercell vector q^* given by $q^*=\delta b^*-n\varepsilon c^*$, where $\delta=0.21$, $\varepsilon=0.78$. The observed d-spacings were obtained from both a Hagg Guinier camera and STOE Automated Diffractometer. Indexing of the subcell lines, especially for the 020, 022 and 0014 reflections, as greatly assisted by utilisation of the line shape fitting routines on the STOE diffractometer.

Using the procedures adopted successfully for indexing the 2212 phase, the supercell lines were assumed in the first instance to be first order satellites of the most intense subcell lines. Specifically, the line at 3.2135 Å, which appeared as a relatively sharp line, was assumed to be a first order satellite of 115. Depending on the indexing of this satellite, two supercell vectors were possible, given by $q^*=\delta b^*+n\varepsilon c^*$ and $q^*=b^*-n\varepsilon c^*$ with $n=1, 2,\cdots$ For each of these, δ was assumed to be 0.21, with $n=1$ and hence a value of ε was calculated. The next stage was to generate a list of calculated d-spacings for first and second order satellites associated with all possible subcell reflections. Two such lists were produced and compared with the experimental d-spacings. Only one of these listings, corresponding to $q^*=0.21b^*-0.75c^*$, was able to give a successful indexing of the supercell lines. Further trial and error refinment led to values of $\delta=0.21$ and $\varepsilon=0.78$ and all the supercell lines could be successfully indexed, as in table 5. It is noted in table 5, that although many supercell lines are first order satellites, five are second order. Some satellite intensities are fairly strong.

VI. Conclusion

The x-ray powder diffraction patterns of the 2212 and 2223 phase can be indexed using a pseudo-tetragonal subcell, $a=5.408$, $c=30.83$ Å, with a supercell vector q^* given by $q^*=0.21b^*-c^*$ and using an orthorhombic subcell $a=5.410$, $b=5.420$ and $c=37.29$ Å, with $q^*=0.210b^*-0.78c^*$ respectively. The incommensurate component in the b direction, δ, is the same for both phases but on going from 2212 phase the superlattice component in the c direction changes from commensurate ($\varepsilon=1$) to incommensurate($\varepsilon=0.78$).

In the present study, an effective method has been developed for indexing the modulated superstructure in the powder diffraction pattern and it has been shown that many reflections that cannot be indexed using the subcell are not due to impurities but are satellite reflections.

Acknowledgements

This work was supported by the Basic Science Research Insitituted Program, Ministry of Education (1993), Republic of Korea.

References

1. C. Michel, M. Hervieu, M.M. Borel, A. Grandin, F. Deslandes, J. Provost, and B. Raveau, Z. Phys. B68 (1987) 421.
2. R.M. Hazen, C.T. Prewitt, R.J. Angel, N.L. Ross, L.W. Finger, G.B. Hadidacos, D.R. Veblen, P.J. Heaney, P.H. Hor, R.L. Meng, Y.Y. Sun, Y.Q. Wang, Y.Y. Xue, Z.J. Huang,

L. Gao, J. Bech, J. Bechtold, and C.W. Chu, Phys. Rev. Lett. 60 (1988) 1174.
3. M.A. Subramanian, C.C. Torardi, J.C. Calabrese, J. Gopalkrishnan, K.J. Morrisey, T.R. Askew, R.B. Flippen, U. Chowdhry, and A.W. Sleight, Science, 239 (1988) 1015.
4. H. Maeda, Y. Tanaka, M. Fukotami, and T. Asano, Jpn. J. Appl. Phys. 27 (1988) L209.
5. J.M. Tarascon, Y. Le Page, L.H. Greene, B.G. Bagley, P. Barboux, D.M. Hwang, G. W. Hull, W.R. McKinnon, and M. Giround, Phys. Rev. B38 (1988) 2504.
6. M. Onoda, A. Yamamoto, E. Takayama Muromachi, and S. Takekawa, Jpn. J. Appl. Phys. 27(5) (1988) L833.
7. K. Kawaguchi, S. Sasaki, H. Hukaida, and M. Nako, Jpn. J. Appl. Phys. 27(6) (1988) L1015.
8. C.H. Chen, D.J. Werder, S.H. Liou, H.S. Chen, and M. Hong, Phys. Rev. B37(6) (1988) 9834.
9. T.M. Shaw, S.A. Shivashankar, S.J. La Placa, J.J. Cuomo, T.R. McGuire, R.A. Roy, K.H. Kelleher, and D.S. Yee, Phys. Rev. B37 (16) (1988) 9856.
10. J.L. Tallon, R.G. Buckley, P.W. Gilberd, M. R. Presland, I.W.M. Brown, M.E. Bowden, L.A. Christian, and R. Goguel, Nature, 333 (1988) 153.
11. R. Herrera, A. Gomez, P. Schabes-Retchkiman and M. Jose-Yacaman, Supercond. Sci. Technol. 3 (1990) 84.
12. H.W. Zandbergen, Y.K. Huang, M.J.V. Meken, J.N. Li, K. Kadowaki, A.A. Menovsky, G. Van Tendeloo, and S. Amelinckx, Nature, 332 (1988) 620.
13. Y. Matsui, H. Maeda, Y. Tanaka, and S. Horiuchi, Jpn. J. Appl. Phys. 28 (6) (1989) L946.
14. Y. Matsui, S. Takekawa. H. Nozaki, and A. Umezono, Jpn. J. Appl. Phys. 28 (4) (1989) L602.
15. Y. Matsui, H. Maeda, Y. Tanaka, S. Horiuchi, S. Takekawa, E. Takayama Muromachi, A. Umezono, and K. Ibe, JEOL News, 26E (2) (1988) 36.
16. E.A. Hewat, M. Dupuy, P. Bordet, J.J. Capponi, C. Chaillout, J.L. Hodeau, and M. Marezio, Nature, 333 (5) (1988) 53.
17. C.J.D. Hetherington, R. Ramesh, M.A. O' Keefe, R. Kilaas, and G. Thomas, S.M. Green, and H.L. Luo, Appl. Phys. Lett. 53 (11) (1988) 1016.
18. M.D. Kirk, J. Nogami, A.A. Baski, D.B. Mitzi, A. Kapitulink, T.H. Gebale, C.F. Quate, Science, 242 (1988) 1673.
19. Y. Gao, P. Lee, P. Coppens, M.A. Subramanian, A.W. Sleight, Science, 241 (1988) 954.
20. S. Horiuchi, H. Maeda, Y. Tanaka, and Y. Matsui, Jpn. J. Appl. Phys. 27 (1988) L1172.
21. N. Yamamoto, Y. Hirotsu, Y . Nakamura and S. Nagakura, Jpn. J. Appl. Phys. 28 (4) 598.
22. C. Greaves and T. Forgan, Nature, 332 (1988) 305.
23. S.A. Sunshine, T. Siegrist, L.F. Schneemever D.W. Murphy, R.J. Cava, B. Batlogg, R.B. Van Dover, R.M. Fleming, S.H. Glarum, S. Nakahara, R. Farrow, J.J. Krajewskijs, M. Zahurak, J.V. Waszczak, J.H. Marshall, P. Marsh, L.W. Rupp, Jr., and W.F. Peck, Phys. Rev. B38 (1988) 893.
24. E.A. Hewat, J.J. Capponi and M. Marezio, Physica, C157 (1989) 502.
25. J.M. Tarascon, Y. Le Page, P. Barboux, B. G. Bagley, L.H. Greene, W.R. McKinnon, G.W. Hull, M. Giround, and D.M. Hwang, Phys. Rev. B37 (16) (1988) 9382.
26. J.L. Tallon, R.G. Buckley, P.W. Gilberd, and M.R. Presland, Physica, C, 158 (1989) 247.
27. H. Nobumasa, T. Arima, K. Shimizu, Y. Otsuka, Y. Murata and T. Kawai, Jpn. J. Appl. Phys. 28 (1) (1989) L57.
28. P.M. David and L.S. Robert, Powder Diffraction 5 (1) (1990) 8.
29. H.W. Zandbergen, P. Groen, G. Van Tendeloo, J. Van Landuyt, and S. Amelinckx, Solid State Commun. 66 (4) (1988) 397.